

Catalysis Science & Technology

Accepted Manuscript



This article can be cited before page numbers have been issued, to do this please use: W. Yu, D. Zhang, X. Guo, C. Song and Z. Zhao, *Catal. Sci. Technol.*, 2018, DOI: 10.1039/C8CY01326H.



This is an Accepted Manuscript, which has been through the Royal Society of Chemistry peer review process and has been accepted for publication.

Accepted Manuscripts are published online shortly after acceptance, before technical editing, formatting and proof reading. Using this free service, authors can make their results available to the community, in citable form, before we publish the edited article. We will replace this Accepted Manuscript with the edited and formatted Advance Article as soon as it is available.

You can find more information about Accepted Manuscripts in the [author guidelines](#).

Please note that technical editing may introduce minor changes to the text and/or graphics, which may alter content. The journal's standard [Terms & Conditions](#) and the ethical guidelines, outlined in our [author and reviewer resource centre](#), still apply. In no event shall the Royal Society of Chemistry be held responsible for any errors or omissions in this Accepted Manuscript or any consequences arising from the use of any information it contains.



Journal Name

ARTICLE

Enhanced Visible light photocatalytic nonoxygen coupling of amines to imines integrated with hydrogen production over Ni/CdS Nanoparticles†

Received 00th January 20xx,
Accepted 00th January 20xx

DOI: 10.1039/x0xx00000x

www.rsc.org/

Weiwei Yu,^a Di Zhang,^a Xinwen Guo,^a Chunshan Song,^{a,b} Zhongkui Zhao^{a,*}

This work presents an efficient strategy for visible light driven imines production through photocatalytic nonoxygen coupling reaction of diverse amines dramatically boosted by hydrogen evolution over the noble-metal free Ni/CdS nanoparticles. Thanks to the integrating effect, close to 100% conversion of benzylamine (75.2 h^{-1} of turnover frequency), 97% selectivity of imine with $21.4 \text{ mmol g}^{-1} \text{ h}^{-1}$ of hydrogen evolution rate ($\lambda > 420 \text{ nm}$) and 11.2% apparent quantum yield (450 nm, 10 mg catalyst) have been achieved at room temperature and ambient pressure. In comparison with the use of common sacrificial agents like TEOA or $\text{Na}_2\text{S}/\text{Na}_2\text{SO}_3$, by using coupling of amines to imines, the H_2 evolution rate increases two orders of magnitude. The aforementioned integrating strategy has been extended to diverse amines, and the outstanding photocatalytic performance for H_2 and imines production was obtained. Besides, the catalyst can be recycled several times without visible activity loss, suggesting a bright perspective for sustainable chemistry and solar utilization. This new discovery may open a new horizon for efficiently boosting solar hydrogen evolution and simultaneously clean producing diverse high value-added fine chemicals under mild conditions.

1. Introduction

Solar-driven hydrogen evolution from water splitting via semiconductive photocatalyst systems is an attractive and sustainable strategy to mitigate environmental issues and meet the increasing demands for energy.¹ Great efforts have been devoted to exploiting highly solar water splitting systems over several decades. However, most semiconductor photocatalysts suffer from a low H_2 evolution efficiency due to the rapid recombination of photo-induced electrons and holes before the electrons migrating to the surface of catalysts for aqueous protons reducing reactions. In order to restrain the recombination of photogenerated electron-hole pairs, noble metals such as Pt, are always used as cocatalysts. Although the noble metals could boost the H_2 evolution efficiency, due to their scarcity and high cost, it is very important to develop noble-metal-free catalysts system.² In addition, the water

oxidation half-reaction to produce O_2 can cause negative aspects in achieving effective hydrogen evolution: (1) The H_2 evolution half reaction is suppressed because of the O_2 is a good electron acceptor. (2) The system-damaging reactive oxygen species can form through uncontrolled O_2 reduction, and most of the hydrogen evolution catalysts are O_2 sensitive.³ (3) The separation process of H_2 and O_2 increases energy consumption and limits commercial value of photocatalytic H_2 production. To efficiently restrain the oxidation half-reaction and recombination of photogenerated electrons and holes, various hole-scavengers are employed, such as CH_3OH ,⁴ triethanolamine (TEOA),⁵ lactic acid,⁶ ascorbic acid,⁷ $\text{Na}_2\text{S}/\text{NaSO}_3$.⁸ However, such a method not only wastes the oxidation energy of the photo-induced holes but also uses a large amount of sacrificial reagents. Hence, it is desirable to replace the hole-scavengers with valuable organic transformations, which would efficiently boost both H_2 production from water splitting and simultaneously synthesis of high value-added chemicals from organic transformations. Nevertheless, the researches in this area remain extremely rare. Kasap et al⁹ realized the photocatalytic reduction of aqueous protons coupled to alcohol oxidation to aldehydes via using a carbon nitride-molecular Ni catalyst system. Moreover, Han et al¹⁰ successfully integrated H_2 production with the transformation of biomass intermediates to the value-added aldehydes and acids. Very recently, Liu et al^{2b} realized H_2 production coupling with benzylamine oxidation over MOF

^a Address here. State Key Laboratory of Fine Chemicals, PSU-DUT Joint Center for Energy Research, School of Chemical Engineering, Dalian University of Technology, Dalian 116024, China. E-mail: zkzhao@dlut.edu.cn

^b EMS Energy Institute, PSU-DUT Joint Center for Energy Research and Department of Energy & Mineral Engineering, Pennsylvania State University, University Park, Pennsylvania 16802, United States

Electronic Supplementary Information (ESI) available: [details of any supplementary information available should be included here]. See DOI: 10.1039/x0xx00000x

composites with Pt as cocatalyst. Unfortunately, no hydrogen produces while the noble Pt cocatalyst is absent and the incentive effects to hydrogen evolution by benzylamine oxidation is worse than TEOA, besides the increase in hydrogen evolution rate is desirable. It is very necessary to design a more efficient noble-metal free catalyst system to realize the coupling of visible light-driven hydrogen evolution with amines oxidation.

Imines are important and valuable chemicals because of the wide application as versatile intermediates for fine chemicals, pharmaceuticals and agrochemicals.¹¹ Great progress has been made for the imines production in the past decade.¹² From economic and environment-friendly viewpoints, solar-driven coupling of amines to imines using O₂ as oxidant has been regarded as a promising approach. To date, various catalysts including supported Au catalysts on TiO₂¹³ or Au-Pd alloy nanoparticles on ZrO₂¹⁴, composite catalysts based on g-C₃N₄¹⁵, Nb₂O₅¹⁶, WS₂¹⁷, WO₃¹⁸ and BiOBr¹⁹ have been developed to promote the photocatalytic aerobic oxidative coupling reactions (Table S1). However, in the aforementioned photocatalytic coupling systems, O₂ is indispensable because the superoxide radicals play a crucial role during the oxidative coupling strategy of amines to imines. The aerobic oxidative coupling of amines to imines is inevitably suffered from a risk of handling an explosive mixture containing flammable organic compounds and O₂, which seriously limits the industrial applications. Moreover, this aerobic oxidative coupling strategy cannot be performed in anaerobic environment such as reductive atmosphere or anaerobic bacteria breed. Therefore, there is an urgent demand for developing an efficient strategy to initiate a nonoxygen coupling of amines to imines.

Herein, we reported that visible light-driven H₂ evolution from water splitting integrating with nonoxygen coupling of amines to their corresponding imines over the Ni/CdS photocatalyst without using of noble metal. Owing to the integrating effect between the two transformations, the excellent H₂ evolution rate and conversion of benzylamine have been achieved under visible light irradiation. The H₂ evolution rate boosting with benzylamine oxidation is two orders of magnitude more than the traditional holescavengers (TEOA or Na₂S/NaSO₃). The maximum hydrogen evolution rate of 21.4 mmol h⁻¹ g⁻¹ and 11.2% optimized apparent quantum yield (450 nm, only 10 mg catalyst being used) associated with 100% conversion of benzylamine have been achieved at room temperature and ambient pressure. This integrating strategy concerning H₂ generation from water splitting associated with the nonoxygen coupling of benzylamine to imine has been successfully extended to diverse amines. Moreover, this research may open a new window to simultaneously boosting both solar hydrogen evolution and the production of diverse high value-added chemicals under mild conditions.

2. Experimental

2.1 Chemicals

Cadmium acetate ((CH₃COO)₂Cd·2H₂O), nickel chloride hexahydrate (NiCl₂·6H₂O), Cobalt chloride hexahydrate (CoCl₂·6H₂O) and thioacetamide were purchased from Tianjin Guangfu Fine Chemical Research Institute. Urea and Iron chloride hexahydrate (FeCl₃·6H₂O) were purchased from Tianjin Damao Chemical Reagent Factory. Ethylene glycol and acetonitrile (CH₃CN) were purchased from Tianjin Fuyu Fine Chemicals Co. Ltd. H₂AuCl₄·4H₂O and H₂PtCl₆·6H₂O were purchased from Shenyang Nonferrous Metal Research Institute. All the chemicals are analytical grade and directly used without further processing. Deionized water was used in all procedures and photocatalytic experiments were implemented under nitrogen atmosphere.

2.2 Preparation of the materials

The CdS NPs were prepared according to the previously reported literature with some modifications.²⁰ Briefly, 2 mmol cadmium acetate (Cd(CH₃COO)₂·2H₂O) and 6 mmol thioacetamide were dissolved in 50 ml ethylene glycol by ultrasonic processing. Above mixed solution was transferred into an 80 ml Teflon-lined autoclave and maintained at 160 °C for 18 h. Next, the autoclave was cooled to room temperature and the orange precipitates were washed three times with deionized water and once with absolute alcohol via centrifugation. The final product was dried at 60 °C in an oven and grinded by using the agate mortar.

The g-C₃N₄ was synthesized by thermal polymerizing of urea under N₂ atmosphere. In detail, 5 g urea was placed in a quartz boat and heated in N₂ flow (30 ml/min) at 550 °C for 4 h with a ramp rate of 5 °C min⁻¹. The light yellow g-C₃N₄ was collected by fully grinding.

The Ni/CdS was prepared by in situ photodeposition in a mixed solution. Typically, 10 mg CdS and 6 μmol NiCl₂·6H₂O contained in 0.15 ml H₂O were dispersed in 2 ml CH₃CN. Above mixed solution was sealed in a flask (10 ml, Synthware) and thoroughly replaced the air by N₂ under stirring. Subsequently, the mixture was irradiated with a 300 W Xe lamp (PLSSXE300/300UV, Perfectlight) with a 420 nm cut-off filter for 5 min. The obtained Ni/CdS was kept in the mixed solution in the flask under N₂ atmosphere and directly used for photocatalytic reactions. Adopted the above method, the Ni/g-C₃N₄ was prepared by replacing CdS with g-C₃N₄, and the Au/CdS, Pt/CdS, Fe/CdS and Co/CdS were obtained by replacing NiCl₂·6H₂O with H₂AuCl₄·4H₂O, H₂PtCl₆·6H₂O, FeCl₃·6H₂O and CoCl₂·6H₂O, respectively. The theoretical loading ratio of metal on CdS or g-C₃N₄ is 3.5 wt %.

2.3. Characterization of materials

Scanning electron microscopy (SEM) images were obtained on a JEOL JSM-5600LV SEM instrument and Transmission electron microscopy (TEM) images were acquired on a JEM-2000EX TEM instrument. X-ray diffraction (XRD) was conducted on a D/Max 2400 diffractometer with monochromatic Cu Kα source. X-ray photoelectron spectroscopy (XPS) measurements were performed on an ESCALAB 250 XPS system with a

monochromatic Al K α X-ray source. The Brunauer-Emmett-Teller (BET) method was utilized to calculate the specific surface area, and the pore size distributions was calculated from an adsorption branch of the isotherm via the Benjamin-Johnson-Hui (BJH) model (3H-2000PS, BeiShiDe Instrument). The UV-vis diffuse reflectance spectra (DRS) were recorded on a JASCO V-550 UV-vis spectrometer.

2.4 Photocatalytic performance test

Typically, 0.15 ml H₂O and 3 ml CH₃CN mixed solution contained 0.5 mmol benzylamine were quickly added into the above Ni/CdS mixed solution in the flask. Then the flask was sealed and thoroughly replaced the air by N₂ under stirring. Subsequently, the mixture was illuminated by the Xe lamp for a certain time with continuous stirring. The reaction temperature was kept at 20 °C by a circulating bath during the experiment process. The generated H₂ was quantified by a gas chromatography (GC 9790 II, FuLi Instruments) equipped with a thermal conductive detector (TCD) and nitrogen as the carrier gas. The organic products were quantified by the GC with a SE-54 capillary column (30 m \times 0.32 mm \times 0.50 μ m), flame ionization detector (FID), argon as the carrier gas and trifluorotoluene as the internal standard. The qualitative analysis of the products was performed by gas chromatography-mass spectrometry (GC-MS, HP6890/5973MSD, Agilent) equipped with a mass spectrometry detector. By similar experimental process, the photocatalytic performance of Ni/CdS nanoparticles for visible light driven nonxygen coupling of diverse amines integrated with H₂ production was measured. TON was calculated on the basis of photodeposited Ni molar amount, while hydrogen evolution rate was obtained based on the dosage of CdS photocatalyst. ¹H nuclear magnetic resonance (NMR) spectra of products were record product was recorded at 25 °C in CD₃CN by a 500 MHz spectrometer (Bruker AVANCE III 500). The cycle experiments were performed by directly adding substrate and H₂O after each cycle. The AQYs were performed similar to the above for photocatalytic performance test while 2.5 mmol benzylamine and 0.5 ml H₂O were added. Different wavelengths of visible light (420, 450, 520 and 600 nm) as light sources were obtained by using band-pass filters. The optimal hydrogen production rate was obtained by measuring the hydrogen yield per 15 mins. Area of irradiation was ca. 6.0 cm². The light intensity was determined by a PL-MW2000 photoradiometer (Perfectlight). The AQY was calculated as follows:

$$\text{AQY} [\%] = \frac{2 \times \text{amount of H}_2 \text{ molecules evolved}}{\text{number of incident photons}} \times 100$$

3. Results and discussion

The CdS nanoparticles (NPs) were synthesized through a facile glycol thermal sulfuration process of cadmium acetate by

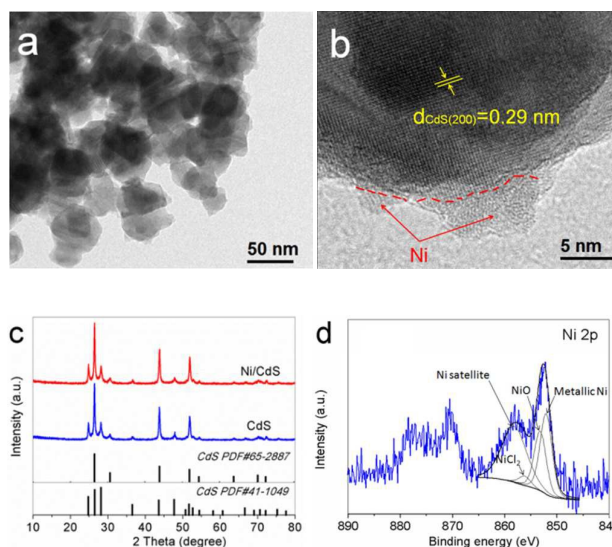
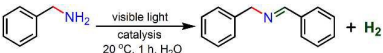


Figure 1. (a) TEM and (b) HRTEM images of Ni/CdS, (c) XRD patterns of CdS and the Ni/CdS, (d) Ni 2p spectra of Ni/CdS.

thioacetamide (see Figure S1a for the SEM image of CdS).²⁰ The metallic Ni NPs were supported on the surface of CdS NPs (Ni/CdS) via an in situ photodeposition method in a mixed solvent (CH₃CN/H₂O) with the NiCl₂·6H₂O as Ni source (Figure S1b for the SEM image of Ni/CdS).²¹ Figure 1a and b show typical transmission electron microscope (TEM) and high-resolution TEM (HRTEM) images of the as-synthesized Ni/CdS catalyst, indicating that the Ni NPs are successfully decorated on the surface of CdS NPs. The X-ray diffraction (XRD) patterns (Figure 1c) confirm that the CdS NPs with a mixed crystalline phases consisting of cubic (PDF#65-2887) and hexagonal (PDF#41-1049) planes. No visible diffraction peaks corresponding to Ni or nickel compounds in the XRD pattern of Ni/CdS can be resolved because of its low loading or amorphous Ni. The chemical states of the elements of Ni/CdS were estimated by X-ray photoelectron spectra (Figure 1d and Figure S2). From Figure 1d, based on references,^{10,21} the fitted peak appearing at 852.1 eV can be assigned to metallic Ni, and the peaks occurring at 853.2 and 856.2 eV can be ascribed to NiO and NiCl₂, respectively. The big peak at around 858.2 eV can be assigned to Ni satellite. The surface area of CdS NPs is 24.2 m² g⁻¹ and the N₂ adsorption-desorption isotherms display type IV isotherms with H3 hysteresis loop suggesting the existence of mesopores (Figure S3a).²² The BJH analysis indicates that CdS NPs owns a wide pore size distribution and the major pore size is centered at 43 nm (Figure S3b), resulting from the accumulation of CdS NPs.

The photocatalytic performance of the as-synthesized Ni/CdS catalyst and the supported diverse metals catalysts on CdS for H₂ production integrated with nonxygen coupling of benzylamine under different reaction conditions are summarized in Table 1. Initially, the photocatalytic activity of Ni/CdS was verified under N₂ atmosphere with visible light irradiation. To our delight, a H₂ production rate of 12.94 mmol h⁻¹ g⁻¹ associated with 94% conversion of benzylamine (45.41

Table 1. Visible light-driven nonoxygen coupling of benzylamine to imine with H₂ Production.^a


Entry	Catalyst	Conv. [%]	Sel. [%]	H ₂ rate [mmol h ⁻¹ g ⁻¹]
1	Ni/CdS	94	96	12.94
2 ^b	Ni/CdS	16	95	1.29
3 ^c	Ni/CdS	-	-	0.02
4 ^d	Ni/CdS	-	-	0.06
5 ^e	Ni/CdS	0	-	0
6	-	0	-	0
7	CdS	8	10	1.73
8	Au/CdS	9	97	0.43
9	Co/CdS	32	85	0.86
10	Pt/CdS	17	94	trace
11	Fe/CdS	4	98	0.09
12	Ni/g-C ₃ N ₄	5	83	trace

[a] Reaction conditions: benzylamine (0.5 mmol), CdS nanoparticle (10 mg), NiCl₂·H₂O (6 μmol), mixed solvent (5 mL CH₃CN/0.3 mL H₂O), nitrogen atmosphere, λ > 420 nm, 1.85 W Xe lamp. The rate of H₂ evolution was calculated for 1 h. [b] CH₃CN as solvent (in absence of H₂O). [c] 0.5 mmol TEOA instead of benzylamine. [d] Na₂S/Na₂SO₃ (0.15 mmol/0.35 mmol) instead of benzylamine and the mixed solvent is 4.15 mL CH₃CN/1.15 mL H₂O. [e] Without light irradiation.

mmol h⁻¹ g⁻¹ of benzylamine oxidation rate) and 96% selectivity of imine are obtained (entry 1), while no transformation takes place under either no visible light irradiation (entry 5) or the absence of Ni/CdS catalyst (entry 6) conditions. From GC-MS spectra of reaction mixture, the main by-products can be confirmed to be dibenzylamine and trace benzaldehyde. The conversion of benzylamine and H₂ production rate dropped sharply in the absence of H₂O under nonoxygen nitrogen atmosphere (entry 2). From Table S1, similar results can be seen over diverse catalysts, the conversion of amines with nonoxygen atmosphere is fall badly compared with aerobic atmosphere. When the benzylamine were replaced with same amount of sacrificial agents as TEOA or Na₂S/Na₂SO₃, H₂ evolution rate decrease two orders of magnitude to 0.02 mmol h⁻¹ g⁻¹ and 0.06 mmol h⁻¹ g⁻¹ (entry 3, entry 4), which indicated that the H₂ evolution stimulating effect of benzylamine is much better than TEOA and Na₂S/Na₂SO₃ which are usual sacrificial agents for photocatalytic H₂ production in our catalytic reaction condition. The result is very different from the H₂ production coupling with selective benzylamine oxidation over MOF composites with Pt cocatalyst.^{2b} In that work, with the same amount of benzylamine as TEOA, H₂ evolution rate decreases from 0.59 mmol h⁻¹ g⁻¹ to 0.33 mmol h⁻¹ g⁻¹. To perform the reaction over individual CdS NPs results in a H₂ production rate of 1.73 mmol h⁻¹ g⁻¹, and only 8% conversion with 10% selectivity for imine (83% of 2-amino-2-phenylacetamide, 7% of dibenzylamine; entry 7). Other supported metal catalysts, such as Au/CdS, Co/CdS, Pt/CdS, and Fe/CdS are less effective than Ni/CdS (entry 8-11). More interestingly, trace H₂ over Pt/CdS catalyst can be generated

(entry 10), although Pt is a well-known cocatalyst for highly-efficient hydrogen evolution reaction from water splitting. Moreover, using g-C₃N₄ as support, only 5% conversion of benzylamine and 85% of imine selectivity with trace H₂ production can be achieved (entry 12). The result indicates Pt cannot effectively abstract hydrogen from substrates which is consistent with previous literature that Pt cannot adsorb hydrogen from alcohol.²³ The aforementioned results strongly suggest that the synergistic effect between metallic Ni and CdS plays a crucial role in improving the photocatalytic performance for coupling of benzylamine to imine with simultaneous hydrogen production from water splitting. Ni serves as active sites for hydrogen evolution on CdS photocatalyst, which promotes the consumption of photogenerated electrons. Moreover, Ni serves as active sites for photocatalytic reaction on CdS photocatalyst, by which not only promotes the migration of photogenerated electrons but also activates substrates.²¹ As a consequence, the synergistic effect between CdS and Ni exists, which efficiently promotes the photocatalytic nonoxygen coupling of amines to imines integrated with hydrogen production over Ni/CdS Nanoparticles. In a word, we unveil an efficient combination strategy for boosting visible light-driven hydrogen evolution from water splitting integrated with nonoxygen coupling of benzylamine to imine over Ni/CdS photocatalyst. The nonoxygen coupling of benzylamine to imine efficiently utilizes photogenerated holes, which boosts the H₂ evolution simultaneously. On the other hand, the consumption of photoinduced electrons by H₂ generation can efficiently inhibit the recombination of photoinduced charge carriers. As a consequence, both H₂ evolution and the benzylamine oxidation are dramatically promoted.

The time courses for H₂ production integrated with the nonoxygen coupling of benzylamine to imine using Ni/CdS NPs are shown in Figure 2a and 2b. The reaction conditions are the same as those described in Table 1 unless otherwise noted. As presented in Figure 2a, the conversion of benzylamine sharp increases with the extending reaction time up to 1 h (94% of conversion with 95 ± 2% of selectivity), and then it begins to slightly increase along with the further extending reaction time. Close to 100 % of conversion and 97 % of selectivity for benzylamine transformation can be obtained for 1.5 h. From Figure 2b, the time course for H₂ production basically agrees with the conversion of benzylamine showed in Figure 2a. It is easily understandable for the increasing H₂ produced volume along with the extending reaction time up to 90 min. More interesting, 21.4 mmol h⁻¹ g⁻¹ of maximum high hydrogen evolution rate at 45 min of reaction time can be obtained. The decreasing hydrogen evolution rate along with the extending reaction time results from the gradually decreasing benzylamine concentration.¹⁰ The apparent quantum yield (AQY) values for H₂ evolution over Ni/CdS photocatalyst under various wavelengths of visible light are demonstrated in Figure 2c. The catalyst owns higher AQY value at 450 nm to be 11.2%. To explore the plausible mechanism of the photocatalytic converting of benzylamine to imine coupled to H₂ production over Ni/CdS NPs, a series of control experiments were

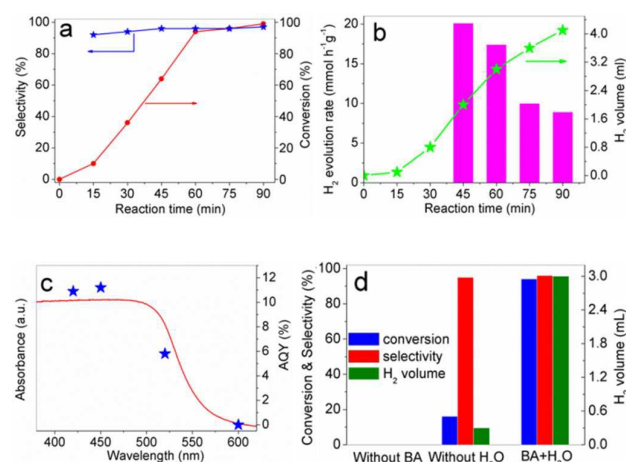
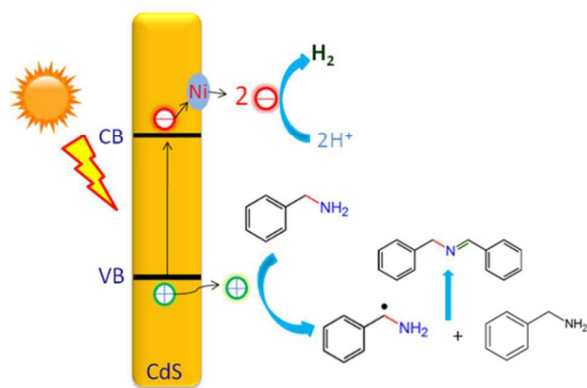


Figure 2. (a) Conversion and selectivity with (b) produced H₂ volume and H₂ evolution rate towards nonoxygen transformation of benzylamine to imine coupled to H₂ production over Ni/CdS catalyst in the presence of H₂O under visible light irradiation. The bars in Figure 2b denote the rate of H₂ evolution averaged over 15 min of visible light irradiation. (c) Ultraviolet-visible diffuse reflectance spectrum of the CdS NPs and wavelength-dependent AQY values towards H₂ evolution over Ni/CdS catalyst (2.5 mmol benzylamine and 0.5 ml H₂O were added). (d) Photocatalytic performance of Ni/CdS under various reaction conditions: BA denotes as benzylamine.

implemented (Table 1 and Figure 2d). No H₂ was detected when benzylamine was absent in the reaction system, which shows clearly the synergistic effect between H₂ production on the Ni cocatalyst and benzylamine conversion plays a critical role in improving the photocatalytic activity of Ni/CdS. Compared with the reaction with adequate H₂O (0.3 mL) added, a much lower photocatalytic activity for converting of benzylamine and rate of hydrogen evolution are obtained in absence of additional H₂O (the crystal water of NiCl₂·6H₂O and acetonitrile solvent containing H₂O provide a spot of H₂O for reaction). The result shows that H₂O is an important reaction component during the catalytic process. On the basis of the above experiment results, a plausible mechanism for photocatalytic nonoxygen strategy for integrating H₂ production with the nonoxygen coupling of benzylamine to



Scheme 1. Plausible reaction mechanism over Ni/CdS nanoparticles under visible light irradiation.

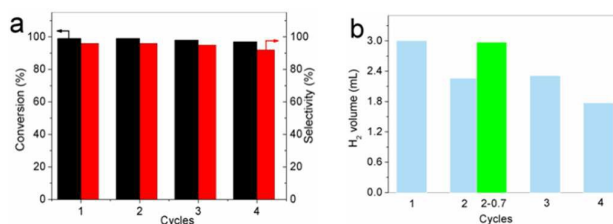


Figure 3. Recyclability in (a) conversion and selectivity as well as (b) the produced H₂ amount for oxygen-free transformation of benzylamine to imine coupled to hydrogen production over Ni/CdS catalyst under visible light irradiation. Reaction conditions: benzylamine (0.5 mmol), CdS nanoparticle (10 mg), NiCl₂·H₂O (6 μmol), mixed solvent (5 mL CH₃CN/0.3 mL H₂O), nitrogen atmosphere, λ>420 nm, 20 °C, 1.5 h. Note: 0.5 mmol of benzylamine was added per cycle experiments (blue bar charts), 0.7 mmol of benzylamine was added (green bar chart).

imine over Ni/CdS with H₂O assistance is proposed and illustrated in Scheme 1. The electrons are excited from the valence band (VB) of CdS to its conduction band (CB) and leave corresponding holes at the VB under light irradiation. The electrons rapidly transfer to Ni NPs and reduce aqueous protons to H₂. The carbon cationic species produced by the holes coupled with benzylamine to produce the desired imine.^{2b} The ratio of H₂ and coupling product towards benzylamine show a good stoichiometric relationship on the basis of the proposed mechanism of reaction (Figure S4).

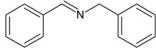
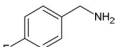
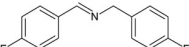
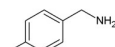
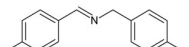
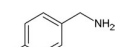
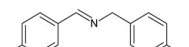
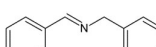
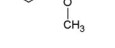
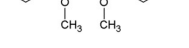
Furthermore, the durability of the as-synthesized Ni/CdS catalyst was tested by cycle experiments. Figure 3 shows the results of visible light-driven nonoxygen coupling of benzylamine to imine integrated with hydrogen evolution in the presence of H₂O. From Figure 3a, no visible decrease in photocatalytic properties for the coupling of benzylamine to imine half-reaction after 4 cycles can be observed. However, the H₂ production half-reaction shows a gradual decline during cycle experiments (blue bar charts; Figure 3b), which is mainly because of part of photoinduced electrons are consumed via reducing Ni²⁺ to Ni due to Ni is easily oxidized when adding substrates during the cycle experiments. However, the H₂ production half-reaction shows a gradual decline during cycle experiments (blue bar charts; Figure 3b), which is mainly because of the Ni on the surface of CdS was easily oxidized (similar to Raney Ni) when adding substrates during the cycle experiments and part of photoinduced electrons are consumed via reducing Ni²⁺ to Ni. The H₂ volume could be regained when the more benzylamine (increase from 0.5 to 0.7 mmol) are used (green bar chart), which further confirms the above supposed reaction mechanism.

After having demonstrated the outstanding photocatalytic performance in nonoxygen coupling of benzylamine to corresponding imine integrated with H₂ evolution under visible light irradiation, we also explored the feasibility of the developed integrating strategy for the transformation of a series of structurally diverse aryl amines (Table 2). The various aryl amines tend to give their corresponding imines with excellent activity and selectivity integrating with outstanding hydrogen evolution activity, suggesting the expandable strategy developed in this work.

ARTICLE

Journal Name

Table 2. Visible light-driven hydrogen production integrating with the nonoxygen coupling of various amines to their corresponding imines over Ni/CdS NPs photocatalyst.^a

No	Substrate	Product	Con. [%]	Sel. [%]	H ₂ [ml]
1b			99	97	4.1
2			98	97	4.1
3			92	96	3.0
4c			90	95	3.1
5			99	95	3.7
6			98	95	4.3
7			96	97	3.3
8			99	95	4.0

[a] Reaction conditions: amines (0.5 mmol), CdS nanoparticle (10 mg), NiCl₂·H₂O (6 μmol), mixed solvent (5 mL CH₃CN/0.3 mL H₂O), 2.0 h, nitrogen atmosphere, λ>420 nm, [b] 1.5 h. [c] 2.5 h.

4. Conclusions

In summary, we have unveiled that H₂ production was dramatically boosted by integrating with nonoxygen coupling of diverse amines to imines over noble-metal free Ni/CdS photocatalyst under visible light irradiation. Thanks to the integrating effect between the two reactions, the catalyst shows high a 99% of high conversion of benzylamine with 97% selectivity of imine for nonoxygen transformation of benzylamine to imine as a probe reaction, associated with 4.1 mL produced H₂, 21.4 mmol g⁻¹ h⁻¹ of maximum hydrogen evolution rate (λ>420 nm) and 11.2% of high apparent quantum yield (450 nm, 10 mg catalyst) for simultaneous hydrogen evolution. Compared with the use of common sacrificial agents like TEOA or Na₂S/Na₂SO₃, by using coupling of amines to imines, the H₂ evolution rate increases two orders of magnitude. The aforementioned integrating strategy has been extended to diverse amines, and the outstanding

photocatalytic performance was obtained. Besides, the catalyst can be recycled several times without visible catalytic activity loss, suggesting a bright perspective for sustainable chemistry and solar utilization. This work not only realizes highly efficient visible light-driven hydrogen evolution integrated with nonoxygen coupling of amines to their imines but also opens a new avenue to integrating highly efficient synthesis of organic chemicals under mild conditions with solar fuel generation.

Conflicts of interest

There is no conflict to declare.

Acknowledgements

This work was financially supported by the National Natural Science Foundation of China (U1610104 and 21676046), the Chinese Ministry of Education via the Program for New Century Excellent Talents in Universities (NCET-12-0079), and the Natural Science Foundation of Liaoning Province (grant no. 2015020200).

Notes and references

- (a) Y. R. Li, Z. W. Wang, T. Xia, H. X. Ju, K. Zhang, R. Long, Q. Xu, C. M. Wang, L. Song, J. F. Zhu, J. Jiang and Y. J. Xiong, *Adv. Mater.*, 2016, **28**, 6959. (b) L. L. Feng, G. T. Yu, Y. Y. Wu, G. D. Li, H. Li, Y. H. Sun, T. Asefa, W. Chen and X. X. Zou, *J. Am. Chem. Soc.*, 2015, **137**, 14023. (c) Z. K. Zhao, G. F. Ge and D. Zhang, *ChemCatChem*, 2018, **10**, 62. (d) C. W. Yang, J. Q. Qin, Z. Xue, M. Z. Ma, X. Y. Zhang and R. P. Liu, *Nano Energy*, 2017, **41**, 1. (e) Y. P. Yuan, L. W. Ruan, B. James, S. C. Joachim-Loo and C. Xue, *Energy Environ. Sci.*, 2014, **7**, 3934.
- (a) K. Chang, Z. W. Mei, T. Wang, Q. Kang, S. X. Ouyang and J. H. Ye, *ACS Nano*, 2014, **8**, 7078. (b) H. Liu, C. Y. Xu, D. D. Li and H. L. Jiang, *Angew. Chem. Int. Ed.*, 2018, **57**, 5379. (c) W. T. Xu, P. Ye, L. James, H. F. Zhang, Y. P. Yuan and Z. Q. Lin, *J. Mater. Chem. A*, 2017, **5**, 21669. (d) L. I. Jiang, L. Y. Wang, G. S. Xu, L. Gu and Y. P. Yuan, *Sustainable Energy Fuels*, 2018, **2**, 430.
- (a) D. R. Sun, L. Ye and Z. H. Li, *Appl. Catal. B: Environ.*, 2015, **164**, 428. (b) W. Lubitz, H. Ogata, O. Rüdiger and E. Reijerse, *Chem. Rev.*, 2014, **114**, 081.
- (a) M. Zhu, S. Kim, L. Mao, M. Fujitsuka, J. Zhang, X. Wang and T. Majima, *J. Am. Chem. Soc.*, 2017, **139**, 13234. (b) S. Guo, Z. Deng, M. Li, B. Jiang, C. Tian, Q. Pan and H. Fu, *Angew. Chem. Int. Ed.*, 2016, **55**, 1830. (c) T. Simon, N. Bonchonville, M. J. Berr, A. Vaneski, A. Adrovic, D. Volbers, R. Wyrwich, M. Döblonger, A. S. Susha, A. L. Rogach, F. Jäckel, J. K. Stolarczyk and J. Feldmann, *Nat. Mater.*, 2014, **13**, 1013.
- (a) Q. Han, B. Wang, J. Gao and L. Qu, *Angew. Chem. Int. Ed.*, 2016, **55**, 10849. (b) D. Zhang, Y. Guo and Z. Zhao, *Appl. Catal. B: Environ.*, 2018, **226**, 1.

- 6 J. Xu, W. M. Yang, S. J. Huang, H. Yin, H. Zhang, P. Radjenovic, Z. L. Yang, Z. Q. Tian and J. F. Li, *Nano Energy*, 2018, **49**, 363.
- 7 H. Lv, T. Ruberu, V. Fleischauer, W. Brennessel, M. Neidig and R. Eisenberg, *J. Am. Chem. Soc.*, 2016, **38**, 11654.
- 8 G. X. Zhao, Y. B. Sun, W. Zhou, X. K. Wang, K. Chang, G. G. Liu, H. M. Liu, T. Kako and J. H. Ye, *Adv. Mater.*, 2017, **29**, 1703258.
- 9 H. Kasap, C. A. Caputo, B. C. M. Martindale, R. Godin, V. W. H. Lau, B. V. Lotsch, J. R. Durrant and E. Reisner, *J. Am. Chem. Soc.*, 2016, **138**, 9183.
- 10 G. Q. Han, Y. H. Jin, R. A. Burgess, N. E. Dickenson, X. M. Cao and Y. J. Sun, *J. Am. Chem. Soc.*, 2017, **139**, 15584.
- 11 (a) J. Gawronski and N. Wascinska, *Chem. Rev.*, 2008, **108**, 5227. (b) L. Greb and J. M. Lehn, *J. Am. Chem. Soc.*, 2014, **136**, 13114. (c) Z. Zhang, F. Wang, M. Wang, S. T. Xu, H. J. Chen, C. F. Zhang and J. Xu, *Green Chem.*, 2014, **16**, 2523.
- 12 (a) B. Chen, S. S. Shang, L. Y. Wang, Y. Zhang and S. Gao, *Chem. Commun.*, 2016, **52**, 481. (b) B. Chen, L. Y. Wang, W. Dai, S. S. Shang, Y. Lv and S. Gao, *ACS Catal.*, 2015, **5**, 2788. (c) J. Xu, R. Q. Zhuang, L. L. Bao, G. Tang and Y. F. Zhao, *Green Chem.*, 2012, **14**, 2384. (d) M. Tamura and K. Tomishige, *Angew. Chem. Int. Ed.*, 2015, **54**, 864.
- 13 (a) S. Naya, K. Kimura and H. Tada, *ACS Catal.*, 2012, **3**, 10. (b) H. Chen, C. Liu, M. Wang, C. Zhang, N. Luo, Y. Wang, H. Abroshan, G. Li and F. Wang, *ACS Catal.*, 2017, **7**, 3632.
- 14 S. Sarina, H. Zhu, E. Jaatinen, Q. Xiao, H. Liu, J. Jia, C. Chen and J. Zhao, *J. Am. Chem. Soc.*, 2013, **135**, 5793.
- 15 (a) H. Wang, X. S. Sun, D. D. Li, X. D. Zhang, S. C. Chen, W. Shao, Y. P. Tian and Y. Xie, *J. Am. Chem. Soc.*, 2017, **139**, 2468. (b) F. Z. Su, S. C. Mathew, L. Möhlmann, M. Antonietti, X. C. Wang and S. Blechert, *Angew. Chem. Int. Ed.*, 2011, **50**, 657. (c) A. Kumar, P. Kumar, C. Joshi, S. Ponnada, A. K. Pathak, A. Ali, B. Sreedhar and S. L. Jain, *Green Chem.*, 2016, **18**, 2514. (d) S. Samanta, S. Khilari, D. Pradhan and R. Srivastava, *ACS Sust. Chem. Eng.*, 2017, **5**, 2562.
- 16 S. Furukawa, Y. Ohno, T. Shishido, K. Teramura and T. Tanaka, *ACS Catal.*, 2011, **1**, 1150.
- 17 F. Raza, J. H. Park, H. R. Lee, H. I. Kim, S. J. Jeonb and J. H. Kim, *ACS Catal.*, 2016, **6**, 2754.
- 18 (a) N. Zhang, X. Li, Y. Liu, R. Long, M. Li, S. Chen, Z. Qi, C. Wang, L. Song, J. Jiang and Y. Xiong, *Small*, 2017, **13**, 17354. (b) N. Zhang, X. Li, H. Ye, S. Chen, H. Ju, D. Liu, L. Yue, W. Ye, C. Wang, Q. Xu, J. Zhu, L. Song and Y. Xiong, *J. Am. Chem. Soc.*, 2016, **138**, 8928.
- 19 A. J. Han, H. W. Zhang, G. K. Chuah and S. Jaenicke, *Appl. Catal. B: Environ.*, 2017, **219**, 269.
- 20 D. Lang, Q. J. Xiang, G. H. Qiu, X. H. Feng and F. Liu, *Dalton Trans.*, 2014, **43**, 7245.
- 21 Z. G. Chai, T. T. Zeng, Q. Li, L. Q. Lu, W. J. Xiao and D. S. Xu, *J. Am. Chem. Soc.*, 2016, **138**, 10128.
- 22 F. He, G. Chen, Y. G. Yu, Y. S. Zhou, Y. Zheng and S. Hao, *Chem. Commun.*, 2015, **51**, 425.
- 23 Z. Jin, Q. Li, X. Zheng, C. Xi, C. Wang, H. Zhang, L. Feng, H. Wang, Z. Chen, Z. J. Jiang, *Photochem. Photobiol.*, A, 1993, **71**, 85.

Enhanced Visible light photocatalytic nonoxygen coupling of amines to imines integrated with hydrogen production over Ni/CdS Nanoparticles†

Weiwei Yu,^a Di Zhang,^a Xinwen Guo,^a Chunshan Song,^{a,b} Zhongkui Zhao,^{a,*}

^a State Key Laboratory of Fine Chemicals, PSU-DUT Joint Center for Energy Research, School of Chemical Engineering, Dalian University of Technology, Dalian 116024, China.
E-mail: zkzhao@dlut.edu.cn

^b EMS Energy Institute, PSU-DUT Joint Center for Energy Research and Department of Energy & Mineral Engineering, Pennsylvania State University, University Park, Pennsylvania 16802, United States

Nonoxygen coupling of amines to imines smoothly takes place initiated by hydrogen evolution over Ni/CdS nanoparticles with visible light. Thanks to the integrating effect between the nonoxygen coupling of benzylamine and the solar-driven reduction of aqueous protons, the outstanding catalytic performance was achieved. The integrating strategy has been extended to coupling of diverse amines to their corresponding imines.

